

Population of analogs of excited states in $^{63}\text{Cu}(p, n)$ at 16, 19, and 22 MeV[†]

C. Wong, V. R. Brown, J. D. Anderson, J. C. Davis, S. M. Grimes, and C. H. Poppe*

Lawrence Livermore Laboratory, Livermore, California 94550

V. A. Madsen

Oregon State University, Corvallis, Oregon 97331

(Received 15 August 1974)

The $^{63}\text{Cu}(p, n)$ analog and excited analog differential cross sections have been measured at bombarding energies of 16, 19, and 22 MeV. Analogs of excited states populated by the (p, n) reaction in medium mass odd- A nuclei have not been previously reported. Coupled-channel calculations for the (p, n) reaction to the $\frac{5}{2}^-$ and $\frac{7}{2}^-$ excited analog states give differential cross sections at 19 and 22 MeV in excellent agreement with measurements. At 16 MeV, the measured $\frac{5}{2}^-$, $\frac{7}{2}^-$, and $\frac{1}{2}^-$ cross sections are higher than calculations at the middle angles, perhaps reflecting the contribution from preequilibrium processes. At 16 and 19 MeV the $\frac{1}{2}^-$ angular distribution shapes suggest some spin-flip contribution. The calculated cross section for the $\frac{1}{2}^-$ state is too high at 22 MeV. As in even- A nuclei a two-step mechanism is mainly responsible for the population of excited analog states in $^{63}\text{Cu}(p, n)$.

NUCLEAR REACTIONS $^{63}\text{Cu}(p, n)$ $E = 16, 19, \text{ and } 22$ MeV; $^{64}\text{Zn}(p, n)$ $E = 22$ MeV; measured $\sigma(\theta)$ for ground-state analog and excited-state analog transitions. Isotopically separated targets. Measurements are compared with coupled-channel calculations.

INTRODUCTION

In addition to the excitation of ground-state analogs in the (p, n) reaction,¹ the sizable population of excited 2^+ analog states² due to the two-step mechanism³ is seen on even- A target nuclei. Except for light mirror nuclei, excited analog states have not been reported on odd- A targets. It has not been clear whether there is a mechanism inhibiting the excitation of these states in odd nuclei or whether the collective strength is spread over too many states to be measurable. Assuming the general validity of the two-step mechanism, a particularly favorable case for the observation of excited-analog states in medium-mass odd- A nuclei is the reaction $^{63}\text{Cu}(p, n)$. The $\frac{1}{2}^-$, $\frac{5}{2}^-$, and $\frac{7}{2}^-$ states are strongly excited in inelastic scattering. Hence the analogs of these states should also be strongly populated in the (p, n) reaction via the two-step mechanism. Moreover, the $B(E2)$ values for these states in ^{63}Cu are consistent with a weak coupling description,⁴ the $\frac{1}{2}^-$, $\frac{5}{2}^-$, and $\frac{7}{2}^-$ states being formed by the coupling of the odd $p_{3/2}$ nucleon to the 2^+ excited core. Time-of-flight measurements indeed show that the $\frac{1}{2}^-$, $\frac{5}{2}^-$, and $\frac{7}{2}^-$ excited-analog states in ^{63}Zn are populated in the $^{63}\text{Cu}(p, n)$ reaction. In this paper the results of these measurements are compared with coupled-channel calculations.

EXPERIMENTAL METHOD

The experimental method is identical to that described previously.⁵ The ^{63}Cu and ^{64}Zn targets were self-supporting metal foils of areal density 4.1 and 4.96 mg/cm², respectively. The isotopic purity of the targets was greater than 99%. The number of detectors was increased from 10 to 16; the angles of observation were 3.5, 9.2, 16.7, 23.8*, 32.3, 38.7, 46.3, 53.7, 61.4*, 68.7, 83.4, 98.7*, 113.2, 128.7*, 143.9, and 159°*. The starred angles denote locations of large detectors, 5.1-cm long by 11.4-cm diameter NE 213 scintillators, compared to 5.1-cm by 5.1-cm detectors for the other angles. The detection efficiencies of the large scintillators were measured relative to the small detectors by bombarding a deuterium gas cell with 8- and 10-MeV deuterons. For 1.6-, 2.5-, 3.5-, and 5.4-MeV recoil proton detector biases and neutrons up to 12 MeV, the measurements show that the product of area and detection efficiency for the large scintillators is uniformly higher than that of the small scintillators by a factor of 5.23 ± 0.17 , which is close to the area or volume ratio of 5.06. This deduced constant detection efficiency is not unexpected since neutrons are incident along the axis of the cylindrical detectors. The ratio of the primary (n, p) scattering probability in the two detectors is proportional to

the area or volume ratio. Multiple collisions with the neutron scattered through 90° by carbon and then by hydrogen, which would enhance the efficiency of the large detectors, are very improbable. The detection efficiency determination for the small NE 213 scintillators and the use of a ^{22}Na source to set the 3.5- and 5.4-MeV detector biases have been discussed previously.⁵ The 1.6- and 2.5-MeV biases correspond respectively in pulse height to the Compton edge and twice the Compton edge of the annihilation radiation from a ^{22}Na source.

The 16- and 19-MeV measurements were made employing a 3.5-MeV bias and $f/5$ sweeping,⁵ which eliminated four out of five beam pulses from the cyclotron. The 22-MeV measurements employed a 5.4-MeV bias and $f/7$ sweeping. At 19 MeV there was some overlap of the low-energy neutrons with high-energy neutrons from the next cycle. This introduces some uncertainty in the level of the continuum neutron spectra but essentially no uncertainty in the analog and excited analog (p, n) cross sections.

To double the counts for analysis, single rather than double display was used.⁵ Time calibration of the system was obtained by accumulating a random time spectrum using a radioactive source and computing the time difference between the γ rays from the target and the analog state neutron group. The ground-state analog neutron group in $^{63}\text{Cu}(p, n)$ was sufficiently pronounced to enable a direct summing of counts from the time spectra to obtain differential cross sections. Because of the smaller cross sections, the ^{63}Cu and $^{64}\text{Zn}(p, n)$ excited-state analog cross sections were obtained using a more sophisticated procedure. The time spectra were converted to energy spectra and the data averaged pairwise. The cross sections were extracted by fitting the background and the resolution function obtained from the ground-state analog group to the various neutron groups. In all cases the centroid of these neutron groups coincided with the expected positions for the excitation of the $\frac{1}{2}^-$, $\frac{5}{2}^-$, and $\frac{7}{2}^-$ levels in ^{63}Zn and the 2^+ level in ^{64}Ga .

EXPERIMENTAL RESULTS

Figure 1 displays the differential energy spectra for $^{63}\text{Cu}(p, n)$ observed at 23.8° for a bombarding energy of 19 MeV. The ground-state analog occurs at an excitation energy U of ~ 5.3 MeV in ^{63}Zn . Although the 1.33- and 1.41-MeV neutron groups in ^{63}Zn were not resolved, the contamination by the 1.41-MeV level is believed to be small since this level is weakly excited in (p, p') scattering on ^{63}Cu ,⁶ and hence its analog is also weakly excited

by the two-step process in the (p, n) reaction. The same arguments are applicable for the 1.55-MeV level, and indeed Fig. 1 confirms that this level is not strongly populated in the (p, n) reaction.

Also shown in Fig. 1 is the method of generating the resolution function: the ground-state analog neutron group (minus background) was reduced by a factor of 8 (see crosses). Since the time widths of the ground state analog and prominent $\frac{7}{2}^-$ excited-state analog neutron groups were found at all bombarding energies to be the same within statistics as the γ -ray (proton) burst width, this resolution function must be corrected for the $(E_n)^{3/2}$ width dependence, where E_n is the laboratory neutron energy, before it can be used for unfolding purposes. In Fig. 1, the narrower width for the $\frac{7}{2}^-$ neutron group is consistent with this deduced $(E_n)^{3/2}$ dependence.

The area or peak height of the neutron groups can then be used to obtain the excited-analog differential cross sections. In the present experiment the 2^+ , $\frac{1}{2}^-$, $\frac{5}{2}^-$, and $\frac{7}{2}^-$ cross sections were obtained by comparing the peak height with that of the ground-state analog neutron group and correcting for the $(E_n)^{3/2}$ width dependence. The an-

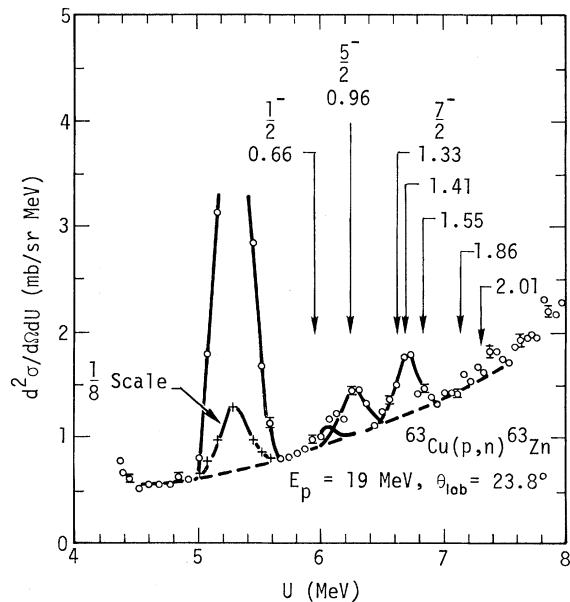


FIG. 1. Differential energy spectra for $^{63}\text{Cu}(p, n)$ at 23.8° and 19-MeV bombarding energy. The arrows indicate the expected positions of the excited analog state neutron groups measured with respect to the ground-state analog. The dashed curve represents the assumed continuum neutron background beneath the analog and excited-analog state neutron groups. The proton burst width was 3.4 ns FWHM and the channel width after averaging was 0.86 ns/channel. The errors are computed from the counting statistics on the individual points before averaging.

gular distributions at 16, 19, and 22 MeV are displayed in Figs. 2, 3, and 4, respectively. At 19 MeV, the $\frac{5}{2}^-$ and $\frac{7}{2}^-$ neutron groups at the forward angles were sufficiently well defined to enable a direct summing of counts from the time spectra. The resulting cross sections were in good agreement with those determined from peak heights. Figures 2, 3, and 4 also display the ground-state analog differential cross sections for $^{63}\text{Cu}(p,n)$ at 16, 19, and 22 MeV, respectively, obtained by

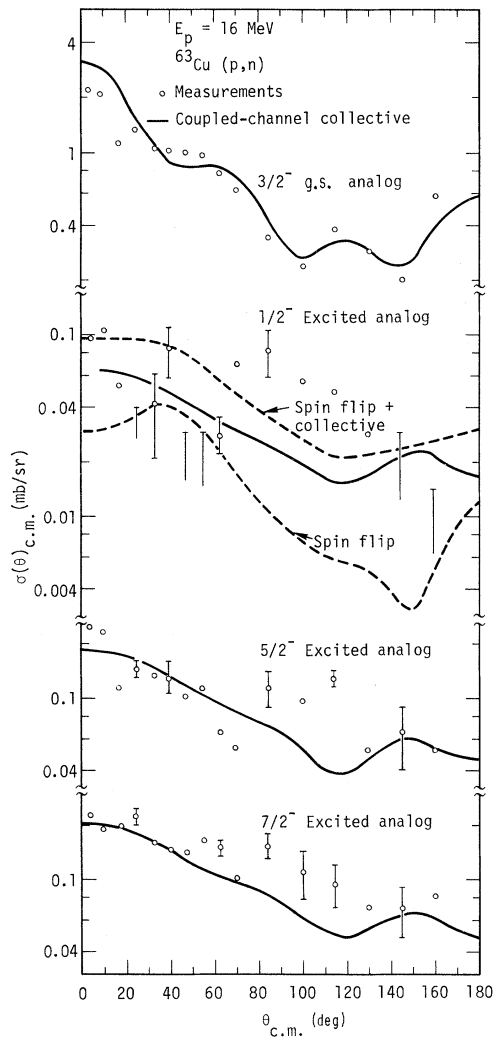


FIG. 2. Measurements and calculations of the ground-state analog and excited-state analog transition in $^{63}\text{Cu}(p,n)$ at 16-MeV bombarding energy. The errors shown are the errors on the peak height determinations, the latter being dependent on the counting statistics in the energy spectra as well as an estimate of the goodness of fit of the line shape to the various neutron groups. Measurements showing only an upper error bar signify that the neutron group was not visible and that the upper error bar is an estimate of the upper limit for this cross section.

summing counts in the time spectra. These differential cross sections agreed with those determined using peak heights normalized at the forward maximum.

THEORY

In a previous paper³ it was shown that the analog of the collective 2^+ first excited state in even nuclei is excited in the (p,n) reaction by the two-step mechanism proceeding through the 2^+ inelastic and 0^+ analog states. The importance of the two-step process for this reaction is due to the fact that the direct inelastic and analog transitions are both strong. In odd- A nuclei the inelastic collective strength is spread over several states, thereby somewhat decreasing the inelastic step

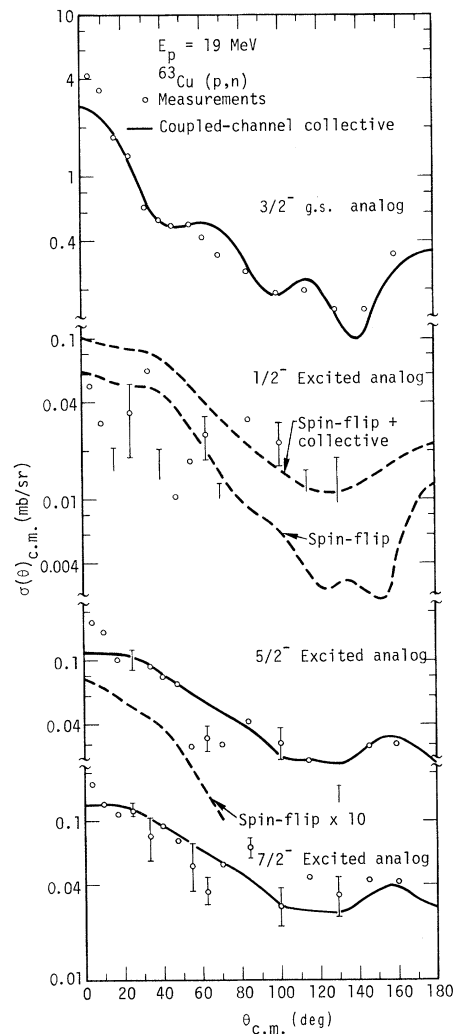


FIG. 3. Measurements and calculations of the ground-state analog and excited-state analog transitions in $^{63}\text{Cu}(p,n)$ at 19-MeV bombarding energy.

for excitation of any particular excited analog state.

Inelastic scattering experiments have demonstrated that for ^{63}Cu the weak-coupling rule for the distribution of the 2^+ strength is approximately correct. In strict weak coupling the $\frac{3}{2}^-$ ground state of ^{63}Cu would couple with the 2^+ core vibration to form a multiplet of collective excited states $\frac{1}{2}^-$, $\frac{3}{2}^-$, $\frac{5}{2}^-$, $\frac{7}{2}^-$, with upward $B(E2)$ strengths proportional to $2J+1$. The $\frac{3}{2}^-$ state has not been identified and the $\frac{5}{2}^-$ state is stronger than expected, but otherwise only small deviations from weak coupling are observed.⁶

Thankappan and True⁷ calculate the low-lying

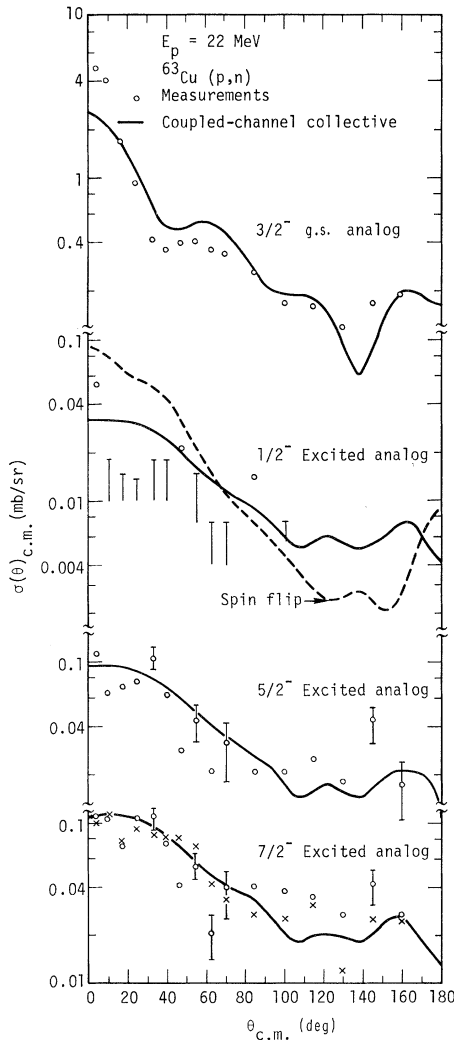


FIG. 4. Measurements and calculations of the ground-state analog and excited-state analog transition in $^{63}\text{Cu}(p, n)$ at 22 MeV. The crosses represent the measured $^{64}\text{Zn}(p, n)$ 2^+ excited-analog cross sections at 22 MeV scaled theoretically, using weak coupling to the $\frac{7}{2}^-$ transition in $^{63}\text{Cu}(p, n)$.

^{63}Cu states in terms of a collective core plus single proton. The eigenstates are then of the form $\psi = \sum C(L, j) |L, j\rangle$ where $L=0, 2$ for the core states and $j = p_{3/2}, p_{1/2}, f_{5/2}$ for the proton. Although the eigenvectors strongly deviate from weak coupling, they still give reasonable agreement with experimental $B(E2)$ values, which are nearly in agreement with weak-coupling ratios for the $\frac{1}{2}^-$, $\frac{5}{2}^-$, and $\frac{7}{2}^-$ members of the 2^+ multiplet. At the same time their results can explain the single-particle strength in these states demanded by stripping experiments.⁸ Their calculated eigenstates also include the $\frac{3}{2}^-$ member of the multiplet, which has a large $|2, p_{3/2}\rangle$ component as in the weak-coupling model. It suffers in inelastic strength from mixture with the $\frac{3}{2}^-$ ground state, although the calculated $B(E2)$ strength still seems too large to be consistent with the inelastic scattering data,⁶ where it is too weak to be identified. The $\frac{1}{2}^-$ state is furthest from weak coupling, being mostly $|0, p_{1/2}\rangle$ but with a sizable $|2, p_{3/2}\rangle$ component.

Accordingly, the excited analog transitions in $^{63}\text{Cu}(p, n)$ are calculated using the Thankappan-True model for the nuclear wave functions of the $\frac{1}{2}^-$, $\frac{5}{2}^-$, and $\frac{7}{2}^-$ members of the 2^+ multiplet. A semiphenomenological procedure is used in which the inelastic strength parameter β and the analog charge exchange strength V_1 are determined from inelastic scattering and quasielastic (p, n) scattering on the same target nucleus. For convenience we couple only four states at a time in the ^{63}Cu and ^{63}Zn system; for example, the $\frac{3}{2}^-$ ground state, $\frac{3}{2}^-$ analog, $\frac{7}{2}^-$ and $\frac{7}{2}^-$ analogs (see Fig. 5). Couplings among excited states are expected to have only a minor effect on the results. In the weak-coupling vibrational model these excited states would not be coupled at all and the coupling is small in the eigenstates of Ref. 7 compared to

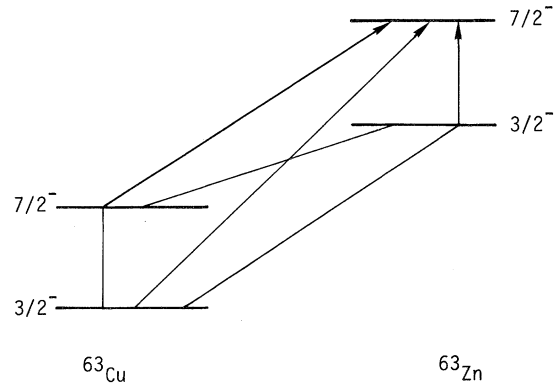


FIG. 5. Schematic diagram showing the two two-step processes contributing to the excitation of the $\frac{7}{2}^-$ state in $^{63}\text{Cu}(p, n)$.

the couplings that are included.

In addition, direct single-particle transitions to the excited analogs must be considered. The $\frac{1}{2}^-$ state is most likely to display this effect, since it appears⁷ to be roughly half $|0, p_{1/2}\rangle$ rather than all $|2, p_{3/2}\rangle$, as in the weak-coupling model. The amplitude for $L=0$ with spin-flip between the large

$|0, p_{3/2}\rangle$ term of the ground state and the $|0, p_{1/2}\rangle$ term of the excited analog should be substantial. Being primarily spin-flip, these cross sections are nearly incoherent with the collective mechanism, and therefore have been calculated separately. The particle spectroscopic amplitudes can be calculated easily from the core-particle

wave function,⁷ and the definition⁹

$$S(J_i J_f I; T_1 T_2 \tau; j_1 j_2) = \langle \psi_f \| A_{IN}(j_1 j_2 \alpha_1 \alpha_2) \| \psi_i \rangle (\hat{I} \hat{\tau})^{-1}, \quad (1)$$

$$A_{IN\rho}(j_1 j_2) = \sum C(j_1 j_2 I; m_1 - m_2 - N) (-1)^{j_1 - m_1} C(\frac{1}{2} \frac{1}{2} \tau; \alpha_1 - \alpha_2 - \rho) (-1)^{1/2 - \alpha_1} \mathcal{Q}_{j_2 n_2 \alpha_2}^\dagger \mathcal{Q}_{j_1 m_1 \alpha_1},$$

where $\mathcal{Q}_{j m \alpha}^\dagger$, $\mathcal{Q}_{j m \alpha}$ are shell-model creation and destruction operators, respectively. Using Eq. (1),

$$S(J_i J_f I; T_i T_f T, j_1 j_2) = \hat{I}^{-1} \sum_{L, J_c} C_f^*(L, j_2) C_i(L, j_1) (-1)^{J_c + I - j_2 - j_1 + T_c + \tau - 1/2 - T_i} \times \hat{J}_i \hat{J}_f \hat{T}_i \hat{T}_f W(j_1 J_i j_2 J_f; J_c I) W(\frac{1}{2} T_i \frac{1}{2} T_f; T_c \tau). \quad (2)$$

For the principal component of the $\frac{3}{2}^- \rightarrow \frac{1}{2}^-$ transition, $|0, p_{3/2}\rangle \rightarrow |0, p_{1/2}\rangle$, this amplitude is 0.9441 compared to 1.1832 for pure particle states coupled to a core of $J_c = 0$, $T_c = 3$.

CALCULATIONS AND RESULTS

The differential cross sections for the (p, n) reaction to the analogs of the $\frac{3}{2}^-$ ground state, $\frac{1}{2}^-$, $\frac{5}{2}^-$, and $\frac{7}{2}^-$ states in ^{63}Cu were calculated with the Oregon-State coupled-channel code.¹⁰ Optical parameters for both neutrons and protons were taken from the global set of Becchetti and Greenlees.¹¹ The inelastic interaction was that of the standard collective model, proportional to the deformation parameter β , and the analog interaction was the $V_1 \vec{T} \cdot \vec{\tau}/A$ term in Ref. 11 with the V_1 strengths scaled by factors of 1.33, 1.01, and 0.931 at energies of 16, 19, and 22 MeV, respectively, to fit the ground-state analog $^{63}\text{Cu}(p, n)$ transition. For ^{63}Cu , the value of $\beta = 0.243$ was used. This value of β and the Thankappan-True eigenvectors give an excellent fit to the 17.5-MeV $^{63}\text{Cu}(p, p')$ $\frac{7}{2}^-$ differential cross section data of McCarthy and Crawley⁶ when the $\frac{3}{2}^-$ ground state, the $\frac{7}{2}^-$ state, and their analogs are coupled. This procedure falls short of fitting the $\frac{3}{2}^-$ inelastic data of Ref. 6 by about 19% and overestimates the $\frac{1}{2}^-$ data by about 2%.

The spin-flip transitions were calculated with the energy-independent effective two-body interaction of Petrovich *et al.*,¹² of which the relevant term for these transitions is a one-Fermi Yukawa interaction with $V_{\sigma\tau} = 12$ MeV. We include a tensor force with a radial form¹³

$$V_T(r) = 3.9 [h_2(i\alpha r) - (\beta^3/\alpha^3) h_2(i\beta r)] \text{ MeV}, \quad (3)$$

where h_2 is a spherical Hankel function and $\alpha = 0.714 \text{ fm}^{-1}$, $\beta = 4 \text{ fm}^{-1}$.

Table I compares the experimental total cross sections with various calculated ones. Spin-flip contributions are given only for the $\frac{1}{2}^-$ excited analog transition because they were found to be negligible for transitions to the other states. Agreement between experiment and theory for the integrated cross sections is satisfactory except for the $\frac{1}{2}^-$ state at 22 MeV, where even the collective contribution exceeds the experimental cross section. Table I shows that the weak-coupling distribution of the collective 2^+ strength for the $\frac{3}{2}^-$ and $\frac{7}{2}^-$ states is well satisfied, in agreement with Ref. 7. The fact that the $\frac{7}{2}^-$ cross section is systematically larger at all energies is inconsistent with the (p, p') results at 17.5 MeV,⁶ although the measured $\frac{5}{2}^-$ and $\frac{7}{2}^-$ integrated cross sections are equal within extreme limits of experimental error.

Figures 2, 3, and 4 show the calculated differential cross sections for the $\frac{3}{2}^-$ ground-state analog and the $\frac{1}{2}^-$, $\frac{5}{2}^-$, and $\frac{7}{2}^-$ excited analog transitions in $^{63}\text{Cu}(p, n)$. As discussed above, V_1 is adjusted to fit the ground-state analog cross section, and the inelastic deformation parameter β was scaled to fit the $\frac{7}{2}^-$ inelastic scattering data of McCarthy and Crawley at 17.5 MeV. The excited analog calculations are then made with no adjustable parameters. The agreement with the magnitude and shape is satisfactory for the (p, n) transition to the $\frac{5}{2}^-$ and $\frac{7}{2}^-$ states. Figure 4 also includes differential cross sections for the $^{64}\text{Zn}(p, n) 2^+$ analog state multiplied by

$$\frac{[\beta(\text{Cu})]^2}{[\beta(\text{Zn})]} \frac{(N-Z)_{\text{Cu}}}{(N-Z)_{\text{Zn}}} \frac{2J_f + 1}{\sum_i 2J_i + 1}$$

to scale it to the weak-coupling model $\frac{7}{2}^-$ excited analog strength [$\beta(\text{Cu})=0.234$, from Ref. 6 and $\beta(\text{Zn})=0.25$, Ref. 14]. Figure 4 shows that the angular distributions for the (p, n) transitions to the $\frac{5}{2}^-$, $\frac{7}{2}^-$, and 2^+ excited analog states are very similar.

DISCUSSION

As in the case of even targets, the odd nucleus ^{63}Cu shows analogs of excited states in the (p, n) reaction. The fact that they have not been reported previously for other medium-mass odd- A nuclei is apparently due to the fractionating of the 2^+ strength among many levels. The two-step mechanism, as in the case of even nuclei, accounts very well for the distribution of strengths in the $^{63}\text{Cu}(p, n)$ spectrum. With the exception of the $\frac{1}{2}^-$ transition, the collective excited analog strength seems to be distributed approximately according to the weak-coupling rules, i.e., proportional to $2J+1$. According to Ref. 7, the $\frac{3}{2}^-$

level of the multiplet occurs with reduced strength at about 2.0 MeV. The peak seen in Fig. 1 is at the right energy, but it seems inconsistent with the (p, p') measurements⁶ that this state should appear with substantial strength in the (p, n) spectrum.

Although in odd nuclei the spin-flip mechanism with $L=0$ becomes possible, it is not expected to be large for a nucleus with a substantial neutron excess.¹⁵ However, in the case of the $^{63}\text{Cu}(p, n)$ reaction, only about $\frac{1}{10}$ of the two-step collective $L=2$ strength goes into the $\frac{1}{2}^-$ transition. Thus, since the $\frac{1}{2}^-$ state has a large $|0, p_{1/2}\rangle$ amplitude, the $L=0$ spin-flip mechanism is competitive. For the $\frac{7}{2}^-$ and $\frac{5}{2}^-$ transitions it is totally negligible (<0.01 of the dominant two-step mechanism). The angular distribution for the excitation of the $\frac{1}{2}^-$ state appears to have a different shape than that of the $\frac{5}{2}^-$ or $\frac{7}{2}^-$ state, which are very similar to each other and to the (p, n) 2^+ excited analog angular distribution, indicating a separate mechanism for the $\frac{1}{2}^-$ case. The spin-flip angular

TABLE I. Integrated cross sections for protons on ^{63}Cu at 16, 19, and 22 MeV. The coupled-channel calculations are compared with measured integrated (p, n) analog and excited-analog cross sections. The Lane potential V_1 is scaled by factors of 1.33, 1.01, and 0.931 at 16, 19, and 22MeV, respectively.

E_p (MeV)	J^π_f	$Q(p, n)$ (MeV)	Cross section (mb)			
			Coupled-channel calculation		Experiment	
			(p, p')	(p, n)	$(p, n)^a$	Exp/Calc.
16	$\frac{3}{2}^-$	-9.58		7.57	7.66 ± 0.54	
	$\frac{1}{2}^-$	-10.25	3.83	0.351	0.61 ± 0.12	1.12 ± 0.22
			(0.194) ^b			
	$\frac{5}{2}^-$	-10.54	10.78	0.953	1.19 ± 0.18	1.25 ± 0.19
19	$\frac{7}{2}^-$	-10.91	12.98	1.11	1.55 ± 0.23	1.40 ± 0.21
	$\frac{3}{2}^-$	-9.58		5.00	5.0 ± 0.35	
	$\frac{1}{2}^-$	-10.25	3.91	0.200	0.28 ± 0.06	0.70 ± 0.14
			(0.199) ^b			
22	$\frac{5}{2}^-$	-10.54	11.10	0.556	0.58 ± 0.09	1.04 ± 0.16
	$\frac{7}{2}^-$	-10.91	13.45	0.649	0.74 ± 0.11	1.14 ± 0.17
	$\frac{3}{2}^-$	-9.58		4.42	4.4 ± 0.31	
	$\frac{1}{2}^-$	-10.25	3.80	0.148	≤ 0.09	≤ 0.27
		(0.188) ^b				
	$\frac{5}{2}^-$	-10.54	10.84	0.419	0.40 ± 0.06	0.95 ± 0.14
	$\frac{7}{2}^-$	-10.91	13.19	0.509	0.55 ± 0.08	1.08 ± 0.16

^a The total cross sections were obtained by graphical integration of smooth curves drawn through the measured points.

^b The value in parentheses represents the spin-flip contribution calculated from the microscopic model and should be added incoherently with the collective contribution for comparison with experiment.

distributions at 16- and 19-MeV show some semblance of this behavior, having a peak at 37° . It is, however, hard to account for the smallness of the state in the spectrum at 22 MeV, since the calculated value of the two-step contribution alone is greater than the measured cross section. In addition, the calculated spin-flip contribution using a constant $V_{\sigma\tau}$ strength is too large. However, better data is needed to verify an energy dependence of $V_{\sigma\tau}$.

The rapid energy dependence of V_1 or V_τ is consistent with a number of other (p, n) analog measurements.^{5, 16} Whatever the cause of this energy dependence,¹⁷ it also is reflected in the excited-analog cross sections since this energy dependent V_1 was used successfully in calculation of the two-step cross section. In fact, from Table I the experimental energy dependence of the $\frac{7}{2}^-$ and $\frac{5}{2}^-$ cross sections is a little faster than that calculated. The excess of experimental over calculated values may be due to preequilibrium nuclear decay. From the angular distributions to the $\frac{5}{2}^-$ and $\frac{7}{2}^-$ states it is seen that the disagreement comes mainly at the middle angles between 60 and 140° . It is greater at the lower energies and the experimental cross sections are more isotropic than the calculated values, as would be expected from a preequilibrium contribution.

In column 7 of Table I the experimental integrated cross sections divided by the calculated values are displayed. These cross section ratios for the $\frac{5}{2}^-$ and $\frac{7}{2}^-$ transitions are greater than one at 16 MeV and equal to one within experimental error at 19 and 22 MeV, consistent with a preequilibrium contribution which decreases with increasing bombarding energy. As discussed above, the experimental cross section for the $\frac{1}{2}^-$ transition is lower than the calculation at 19 and 22 MeV and the discrepancy increases with increasing energy. The similarity of angular distributions for the $\frac{5}{2}^-$ and $\frac{7}{2}^-$ transitions to each other and to that of the 2^+ state in $^{64}\text{Zn}(p, n)$, together with the agreement between theory and experiment for the $\frac{5}{2}^-$ and $\frac{7}{2}^-$ levels support the general picture of the (p, n) reaction proceeding by way of the two-step mechanism, the 2^+ strength being divided among several states.

Note added in proof: The $^{62}\text{Ni}(p, n)$ ground state and 2^+ excited state analog cross sections have recently been measured at bombarding energies of 19 and 22 MeV. The deduced fractionation of the 2^+ strength into the $\frac{7}{2}^-$ excited analog transition in $^{63}\text{Cu}(p, n)$ is 0.4, in excellent agreement with the predictions of the weak coupling and Thankappan-True models.

[†]Work performed under the auspices of the U. S. Atomic Energy Commission.

*On sabbatical leave from the University of Minnesota.

¹J. D. Anderson and C. Wong, Phys. Rev. Lett. 7, 250 (1961); J. D. Anderson, C. Wong, and J. W. McClure, Phys. Rev. 126, 2170 (1962).

²J. D. Anderson and C. Wong, Phys. Rev. Lett. 8, 442 (1962).

³V. A. Madsen *et al.*, Phys. Rev. Lett. 28, 629 (1972).

⁴Amos de-Shalit, Phys. Rev. 122, 1530 (1961); R. L. Robinson, F. K. McGowan, and P. H. Stelson, *ibid.* 134, B567 (1964).

⁵C. Wong, J. D. Anderson, J. C. Davis, and S. M. Grimes, Phys. Rev. C 7, 1895 (1973).

⁶A. L. McCarthy and G. M. Crawley, Phys. Rev. 150, 935 (1966).

⁷V. K. Thankappan and W. W. True, Phys. Rev. 137, B793 (1965).

⁸A. G. Blair, Phys. Rev. 140, B648 (1965); A. G. Blair, Phys. Lett. 9, 37 (1964).

⁹V. A. Madsen, Nucl. Phys. 80, 177 (1966).

¹⁰M. J. Stomp, F. A. Schmittroth, and V. A. Madsen, U. S. Atomic Energy Commission Technical Report Contract No. AT(45-1)-2227, Task Agreement No. 11 (unpublished).

¹¹F. D. Becchetti, Jr., and G. W. Greenlees, Phys. Rev. 182, 1190 (1969).

¹²F. Petrovich, H. McManus, V. A. Madsen, and J. Atkinson, Phys. Rev. Lett. 22, 895 (1969).

¹³F. A. Schmittroth, Ph.D. thesis, Oregon State Uni-

versity, 1968 (unpublished); C. Wong, J. D. Anderson, V. A. Madsen, F. A. Schmittroth, and M. Stomp, Phys. Rev. C 3, 1904 (1971).

¹⁴P. H. Stelson and F. K. McGowan, Nucl. Phys. 32, 652 (1962).

¹⁵V. A. Madsen, in *Proceedings of the Second Conference on Nuclear Isospin, Asilomar-Pacific Grove, California, 1969*, edited by J. D. Anderson, S. D. Bloom, J. Cerny, and W. W. True, (Academic, New York, 1969); V. A. Madsen, in *Nuclear Spectroscopy and Nuclear Reactions*, edited by J. Cerny (Academic, New York, to be published), Chap. IX, p. 300.

¹⁶S. M. Grimes *et al.*, Bull. Am. Phys. Soc. 19, 473 (1974); Phys. Rev. C 11, 158 (1975).

¹⁷It has been pointed out by J. D. Carlson, D. A. Lind, and C. D. Zafiratos [Phys. Rev. Lett. 30, 99 (1973)] that the "isospin conserving" neutron potentials derived from the Becchetti and Greenlees proton potential and experimentally determined isospin potentials give fits to the neutron elastic scattering data of comparable quality to those of the Becchetti and Greenlees neutron potential. A similar conclusion is suggested by G. R. Satchler [*Isospin in Nuclear Physics*, edited by D. H. Wilkinson (North-Holland, Amsterdam, 1969), Chap. 9]. Carlson *et al.* also point out that the isospin conserving potential they deduce fits the neutron reaction cross section data better than the Becchetti and Greenlees neutron potential.

To determine whether the use of the neutron potential of Ref. 11 induces the energy dependence of V_1 , the

coupled-channel calculations were repeated with the isospin conserving neutron potential obtained by changing the signs of the $(N-Z)/A$ terms in the proton potential of Becchetti and Greenlees. With this neutron potential, scaling factors of 1.21 and 0.86 for V_1

were required to fit the $^{63}\text{Cu}(p, n)$ data at 16 and 22 MeV, respectively. These are both about 10% smaller than the corresponding factors obtained with the neutron potential of Ref. 11 but yield the same energy dependence for V_1 .